Fractal analysis of ostracod shell variability: A comparison with geometric and classic morphometrics

GIUSEPPE AIELLO, FILIPPO BARATTOLO, DIANA BARRA, GRAZIANO FIORITO, ADRIANO MAZZARELLA, PASQUALE RAIA, and RAFFAELE VIOLA

Aiello, G., Barattolo, F., Barra, D., Fiorito, G., Mazzarella, A., Raia, P., and Viola, R. 2007. Fractal analysis of ostracod shell variability: A comparison with geometric and classic morphometrics. *Acta Palaeontologica Polonica* 52 (3): 563–573.

Two statistical methods, fractal geometry and geometric morphometrics, are tested for their applicability to ostracod systematics. For this comparison, two morphologically similar ostracod species (*Krithe compressa* and *Krithe iniqua*) whose genus-level systematics is still incompletely resolved, are selected. Twenty-nine right valves of each species were collected from the upper Pliocene samples at the Monte San Nicola section in southern Italy. Statistical analyses (MANOVA on morphometric shape variables, and D values) were utilized to test if geometric morphometrics and fractal analysis are appropriate into discriminating between the two species. Both methods succeeded in distinguishing the species statistically. The fractal analysis of the two ostracod species shows D values centered on 1.31±0.02 for *Krithe iniqua* and on 1.40±0.02 for *Krithe compressa*. Geometric morphometric analysis indicates significant differences between the two species and allows studying intra-populational variability as well as. The most variable traits indicated by geometric morphometrics are vestibular area and posterior outline of the shell, indicating that these traits are the most relevant for the systematics of the species analyzed. Both fractal geometry and geometric morphometrics provide a measure of population variability. Fractal analysis has the advantage of being free from any subjectivity in the selection of characters and could be most appropriate to use for analysis of complex ornamentation for systematic purposes. However, a possible advantage of geometric morphometrics over fractal analysis is its ability to indicate where statistically significant variations in shape occur on the shell.

Key words: Ostracoda, *Krithe*, fractal geometry, geometric morphometrics, morphological variability, systematics.

Giuseppe Aiello [aie64llo@hotmail.com], Filippo Barattolo [lippolo@unina.it], and Diana Barra [dibarra@unina.it], Dipartimento di Scienze della Terra, Università di Napoli "Federico II", Largo S. Marcellino, 10, 80138, Napoli, Italy;
Graziano Fiorito [gfiorito@szn.it], Stazione Zoologica "Anton Dohrn", Villa Comunale, 1-80121 Napoli, Italy;
Adriano Mazzarella [adriano.mazzarella@unina.it] and Raffaele Viola [rafviola@unina.it], Dipartimento di Geofisica e Vulcanologia, Università di Napoli "Federico II", Largo S. Marcellino, 10, 80138 Napoli, Italy;
Pasquale Raia [pasquale.raia@libero.it], Dipartimento S.T.A.T. Università del Molise, Isernia, Via Mazzini 8, 86170, Isernia, Italy.

Introduction

Analysis of morphological variability is one of the fundamental steps for the resolution of taxonomic problems. Assessment of the amount and nature of morphological variability among organisms, both living and fossil, is currently benefiting from mathematical studies that allow statistical analysis of morphological disparity in a given group for a given time-interval.

Several techniques are currently being used to describe and measure morphological variability. However there is no general agreement among researchers on the appropriateness of one method over the others.

The aim of this paper is to compare the relative power and appropriateness of fractal geometry and geometric morphometrics for taxonomy. By attributing a numerical value to a curved line, fractal geometry provides a method of standardisation when trying to distinguish between different species. On the other hand, geometric morphometrics has the advantage of topologically investigating shape variation through thin plate spline visualization, thereby providing a potential connection with the naked-eye approaches of classical systematics.

In requiring a certain number of specimens for statistical analysis, both methods are technically well-suited to the study of fossil species taxonomy, especially of invertebrates and microfossils for which large populations are often available.

This study does not address questions concerning species concepts: natural scientists have discussed the "species problem" extensively, introducing numerous species definitions but without reaching full agreement (Mayden 1997). The use of the morphological (or typological) species concept has been severely criticized by the upholders of the biological species concept (e.g., Mayr 1996) who tend to treat it as an

obsolete notion. Despite this criticism, most paleontologists and many neontologists accept "morphospecies" as a matter of fact in their daily research. For the purpose of this study, some of the modern definitions of morphological species are equally satisfactory. For example, Claridge et al. (1997) defined species as "a community, or a number of related communities, whose distinctive morphological characters are, in the opinion of a competent systematist, sufficiently definite to entitle it, or them, to a specific name". Cronquist (1988) considered species as "the smallest groups that are consistently and persistently distinct and distinguishable by ordinary means."

In the last two decades, the increased use of fractals in the life sciences has led to many applications in different areas of research in biology, palaeontology and related disciplines. Fractal geometry may contribute to the description and better understanding of a large number of phenomena, ranging from the architecture of chromosomes to the structure of bronchial tubes, and from insects movement to population growth rate, that is, virtually everywhere life expresses its complexity (references in Stanley 1992; Nonnenmacher et al. 1994; Kenkel and Walker 1996). The study of the morphology of living and fossil organisms by fractals is still not greatly developed, although some authors have laid the groundwork with the publication of papers on the fractal dimension of, for instance, leaf outlines (Vlcek and Cheung 1986), root systems (Tatsumi et al. 1989), perimeters of algal species (Corbit and Garbary 1995; Davenport et al. 1996) and ammonoid suture lines (Boyajian and Lutz 1992). Vlcek and Cheung (1986) were possibly the first, measuring the fractal dimension of the leaf margins in some tree species and showing the potential of fractal geometry in taxonomy.

Geometric morphometrics can be traced back to D'Arcy Thompson seminal book *On Growth and Form* (1917). Because of the implicit difficulties in the mathematics involved, full-fledged application to systematics is relatively recent (e.g., Reyment 1993, 1995; Reyment and Abe 1995; Elewa 2003, 2004). Since Bookstein's (1989, 1991) thin plate spline method and Rohlf and Slice's (1990) paper on generalised least squares, countless published studies have been added to the bibliography on geometric morphometrics (Adams et al. 2004). Geometric morphometrics has been traditionally used in taxonomic studies (for ostracods, see Reyment 1993, 1995; Reyment and Abe 1995; Elewa 2003). Yet, the recent literature also provides examples of morphofunctional studies (e.g., Bruner and Manzi 2004; Raia 2004; to name just a few of the latest in the field of paleontology).

To achieve the aims of the current paper, two ostracod species belonging to *Krithe* Brady, Crosskey, and Robertson, 1874 have been chosen due to the nature of the shell features of this genus. Species of *Krithe* are characterized by having smooth valves; consequently, the taxonomic features used to differentiate species are essentially internal, mainly located on the inner lamella. *Krithe compressa* (Seguenza, 1880) and *Krithe iniqua* Abate, Barra, Aiello, and Bonaduce, 1993 are similar but distinct species, previously discussed by Abate et al. (1993).

The shape, width and size of the anterior vestibulum, and the pattern of marginal pore canals are generally considered as the most important specific characters. All of these features are best observed in transmitted light. In contrast to the carapace ornament of many ostracod taxa, these features are not well expressed in *Krithe*.

There is general agreement on the degree of variability of these characters; however, different evaluations have been given of their range of variation within a single species. Van den Bold (1968) and Zhou and Ikeya (1992) showed two examples of extremely different approaches: the former figured specimens with rather dissimilar vestibula as *Krithe dolichodeira* Bold, 1946; the latter split two species, *K. antisawanensis* Ishizaki, 1966 and *K. surugensis* Zhou and Ikeya, 1992, on the basis of very minute morphological details.

Despite disagreement about the importance of some features, recent studies attempting to clarify the systematics of various species of *Krithe* (e.g., Abate et al. 1993; Coles et al. 1994; Ayress et al. 1999) have produced encouraging results. The diagnostic criteria accepted in the present paper are the ones used by Abate et al. (1993). It is worth noting that *Krithe* species are usually very diffult to demarkate. This is mostly due to ecophenotypic variation of the diagnostic characters due to environmental factors such as dissolved oxygen, food supply and water depth (Peypouquet 1975, 1977, 1979; Van Harten 1995), although the very nature of these effects is still controversial (McKenzie et al. 1989; Zhou and Ikeya 1992; Whatley and Zhao 1993; Van Harten 1996; Corbari 2004).

In this first attempt, three-dimensional morphological analysis has been found unsuitable due to the complexity of data acquisition. Instead, we have used two-dimensional projections, which are common in studies of the morphology and systematics of *Krithe*. This type of graphical representation—commonly utilized in modern studies in the natural sciences—provides detailed, clear and relatively simple images which prove to be adequate for the aims of the current study.

Institutional abbreviation.—B.O.C., Bonaduce Ostracods Collections, Museo di Paleontologia dell'Università "Federico II" Napoli.

Other abbreviations.—D, fractal dimension; H, maximum height of the shell; K-S, Kolmogorov-Smirnov statistic; L, maximum length of the shell; p, pobability of significance of test statistics; RW, relative warp; SV, single value of relative warp vectors; U, Mann-Whitney statistics.

Fractal areal clustering

The topological (D_T) and Euclidean (D_E) dimensions of geometrical sets assume only the integer values zero, one, two, three (for some sets they can be equal), differently from the fractal dimension D which can assume all the decimal values

between zero and three (Mandelbrot 1983; Fig. 1). The clustering index of a coordinate set can be obtained in a very effective way using the fractal dimension that may be computed through the correlation integral C(R) (Grassberger and Procaccia 1983; Luongo and Mazzarella 1997), which counts the number of pairs with distance $|X_i-X_j|$ smaller than R. This is done by taking each point in turn as a centre and analysing the distribution of the remaining points relative to it. The correlation integral is defined as:

$$C(R) = \frac{2}{N(N-1)} \sum_{i=1}^{N} \sum_{j=1}^{N} \Theta(R - X_i - X_j),\ i \neq j$$

where Θ is the Heaviside function, N is the number of available points and X_i is the co-ordinate set of the ith point. The normalisation factor 2/(N(N–1)) represents the reciprocal of the number of pairs so that C(R) tends to one for R tending to infinite. If the distribution of N points has a fractal structure then:

$$C(R) \sim R^D$$

or, equivalently, on a log-log scaled plane

$$\log(C) \sim D\log(R) \quad (1)$$

C(R) can be considered as the cumulative frequency distribution of all inter-point distances. D indicates the correlation dimension that is a lower bound for the true fractal dimension, although it is generally assumed that the two dimensions are similar (Korvin et al. 1990). Theoretically, fractal sets display a straight line in the log-log plot for virtually any interval of R. However, for experimental data there is a limited scaling region with lower and upper limits, due respectively to the minimum and maximum distance among pairs of co-ordinates: for the minimum distance, values must not be lower than the precision of the data, while for the maximum distance the most important constraint is the size and shape of the region investigated. These considerations lead to an estimation of D from the regression coefficient of the relationship (1), within a specific range of distances, only when the correlation coefficient r among the available n pairs of log(C) and log(R) has a confidence level not lower than 99%. The confidence level is here based on the null hypothesis of zero correlation that is rejected at 99% confidence level when the following relationship

$$\left(r\sqrt{n-2}\right)\left(\sqrt{1-r^2}\right)^{-1}$$

gives a value larger than that provided by the Student t distribution with the number of degrees of freedom equal to 2° and the confidence level 99% (Mazzarella 1998).

To understand fully the problem of a fractal characterisation of a data set, let us compute the correlation integral of an ideal distribution of 225 points uniformly distributed, for example, at a distance of 2 μm over an area of 30 × 30 μm² (Fig. 1). For the computation of C(R), the smallest distance has been chosen to be 2 μm gradually increased by a factor of two. The fractal relationship is found to hold for R between 4 and 16 μm with a D = 2.0. For R greater than 16 μm, that is

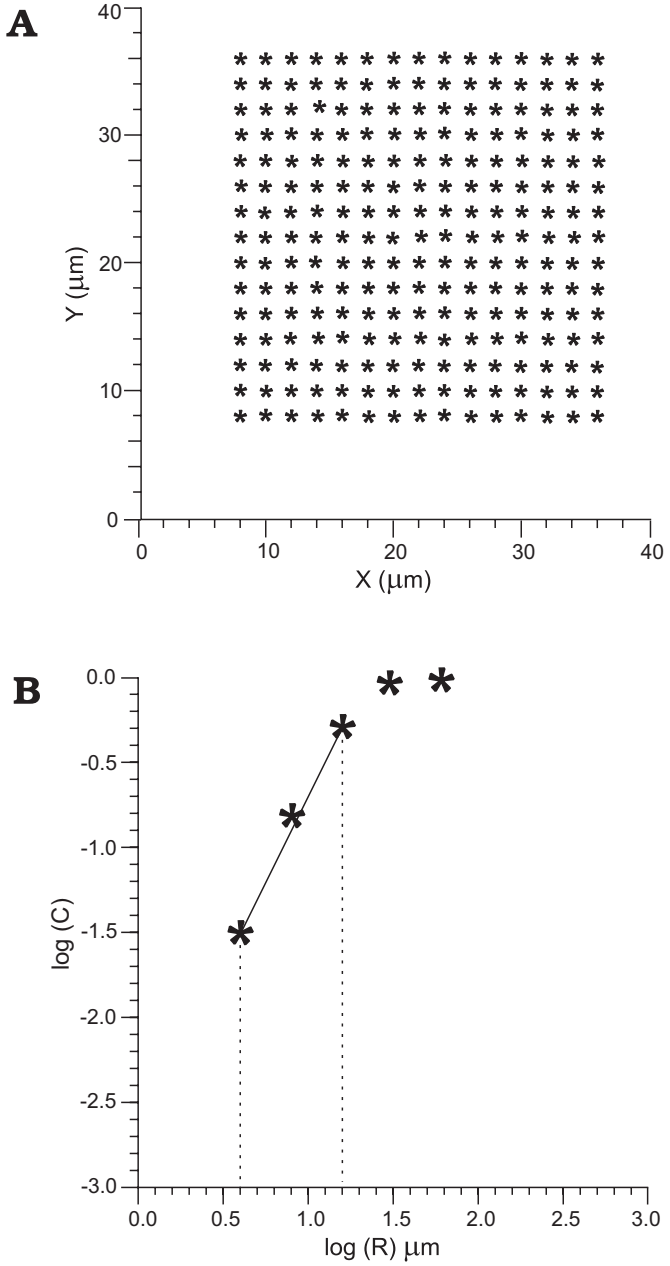

Fig. 1. **A**. Ideal uniform network of 225 points spaced 2 mm apart over an area of 30 × 30 mm². **B**. The log of number of pairs C of the stations, with mutual distance smaller than R, as a function of log(R) (mm); the vertical dashed lines represent the lower (4 mm) and upper (16 mm) limits of R, inside which the linear slope provides the best fitting to the investigated co-ordinates.

equal to about one third of the largest distance, the log-log plot of C(R) is curved. Therefore, a correct interpretation of D requires that values of C(R) for R larger than one third of the entire image size have to be discarded (Dongsheng et al. 1994), in concordance with the rules of spectral analysis applied to time series (Bath 1974). Moreover, the lower limit of the scaling region, here equal to 4 μm, represents the minimum detectable wavelength whose identification requires only three points; it corresponds to two times the gridding area of the investigated data set.

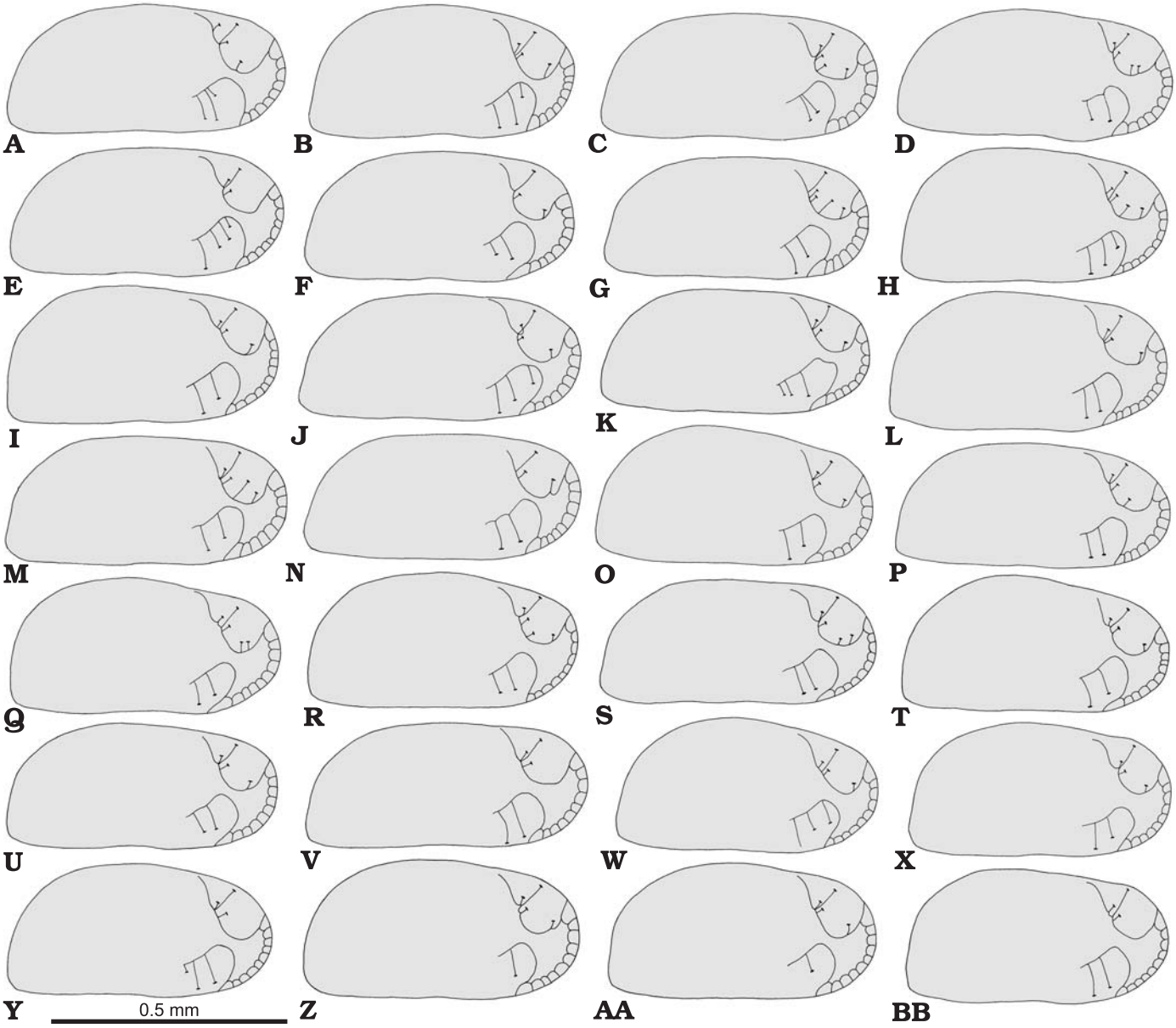

Fig. 2. *Krithe iniqua* Abate, Barra, Aiello, and Bonaduce, 1993, right valves; transparence drawings from external view; sample 59; upper Pliocene. **A**. KI-01, B.O.C. 2490. **B**. KI-02, B.O.C. 2491. **C**. KI-03, B.O.C. 2492. **D**. KI-04, B.O.C. 2493. **E**. KI-05, B.O.C. 2494. **F**. KI-06, B.O.C. 2495. **G**. KI-07, B.O.C. 2496. **H**. KI-08, B.O.C. 2497. **I**. KI-09, B.O.C. 2498. **J**. KI-10, B.O.C. 2499. **K**. KI-11, B.O.C. 2500. **I**. KI-12, B.O.C. 2501. **L**. KI-13, B.O.C. 2502. **M**. KI-14, B.O.C. 2503. **N**. KI-15, B.O.C. 2504. **O**. KI-16, B.O.C. 2505. **P**. KI-17, B.O.C. 2506. **Q**. KI-18, B.O.C. 2507. **R**. KI-19, B.O.C. 2508. **S**. KI-20, B.O.C. 2509. **T**. KI-21, B.O.C. 2510. **U**. KI-22, B.O.C. 2511. **V**. KI-23, B.O.C. 2512. **W**. KI-24, B.O.C. 2513. **Y**. KI-25, B.O.C. 2514. **Z**. KI-26, B.O.C. 2515. **AA**. KI-27, B.O.C. 2516. **BB**. KI-28, B.O.C. 2517.

Materials and data collection

Adult specimens of the ostracod species *Krithe compressa* (Seguenza, 1880) and *Krithe iniqua* Abate, Barra, Aiello, and Bonaduce, 1993, were collected from the upper Pliocene samples of the Monte San Nicola section (Abate et al. 1993; Aiello et al. 2000). The material consists of 29 right valves of *K. iniqua* from sample 59 (KI-01 to KI-29), and 29 right valves of *K. compressa* from samples 50 (7 valves: KC-01 to KC-07), 51 (11 valves: KC-08 to KC-18) and 58 (11 valves: KC-19 to KC-29).

All specimens were observed under transmitted light and drawn by means of a visopan Reichert at a magnification of ×201(successively reduced in Figs. 2, 3). Basically, these drawings depict the lateral outline of the valves and the anterior third of the inner lamella (Fig. 4). The pictures were drawn with a technical pen (line thickness 0.30 mm) on tracing paper.

For each specimen we also measured length (L) and height (H) in mm.

Each drawing was imported using a flatbed scanner and then visualized on a PC monitor in bitmap format. Since the resulting raster image is made of pixels, it was necessary to

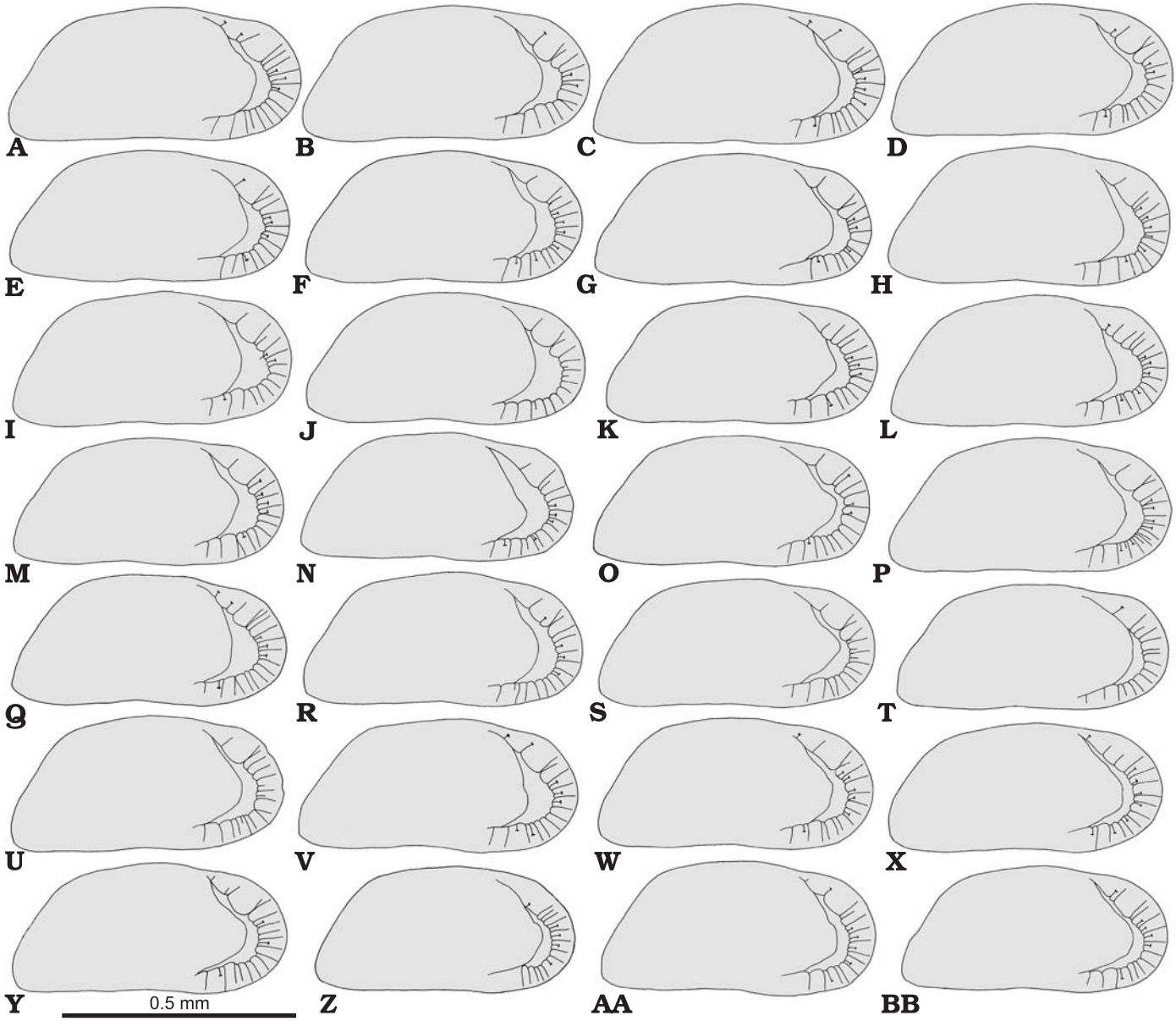

Fig. 3. *Krithe compressa* (Seguenza, 1880), right valves; transparence drawings from external view; sample 50 (**A**–**G**), sample 51 (**H**–**R**), sample 58 (**S**–**BB**); upper Pliocene. **A**. KC-01, B.O.C. 2519. **B**. KC-02, B.O.C. 2520. **C**. KC-03, B.O.C. 2521. **D**. KC-04, B.O.C. 2522.**E**. KC-05, B.O.C. 2523. **F**. KC-06, B.O.C. 2524. **G**. KC-07, B.O.C. 2525. **H**. KC-08, B.O.C. 2526. **I**. KC-09, B.O.C. 2527. **J**. KC-10, B.O.C. 2528. **K**. KC-11, B.O.C. 2529. **L**. KC-12, B.O.C. 2530. **M**. KC-13, B.O.C. 2531. **N**. KC-14, B.O.C. 2532. **O**. KC-15, B.O.C. 2533. **P**. KC-16, B.O.C. 2534. **Q**. KC-17, B.O.C. 2535. **R**. KC-18, B.O.C. 2536. **S**. KC-19, B.O.C. 2537. **T**. KC-20, B.O.C. 2538. **U**. KC-21, B.O.C. 2539. **V**. KC-22, B.O.C. 2540. **W**. KC-23, B.O.C. 2541. **X**. KC-24, B.O.C. 2542. **Y**. KC-25, B.O.C. 2543. **Z**. KC-26, B.O.C. 2544. **AA**. KC-27, B.O.C. 2545. **BB**. KC-28, B.O.C. 2546.

utilise a vector form with a larger amount of details, which is in turn dependent on the size and resolution of the image.

In fact, a vector image is stored as geometric objects, such as lines and arcs drawn between specific coordinates. Vector drawings are largely used in CAD (Computer Aided Design) and GIS (Geographical Informations Systems) and in other applications that require a high standard of accuracy. After many trials, we concluded that a resolution of 300 dpi was sufficiently high to reduce the noise inherent in the digitization process and was appropriate for the spatial resolution of the digitized drawings of the ostracods. A resolution lower than 300 dpi does not provide a sufficient number of data points to obtain reliable fractal dimensions. Moreover, the values of fractal dimensions have been found to be independent of resolution at values higher than 300 dpi.

The vectorization process takes into account the magnification (201×) and the digitization resolution (300 dpi) and transforms the bidimensional projections of ostracod shells into x,y co-ordinates measured in microns.

To quantify the degree of areal clustering of morphological variability of the two ostracod species and to identify the specific range of distances inside which the co-ordinates follow

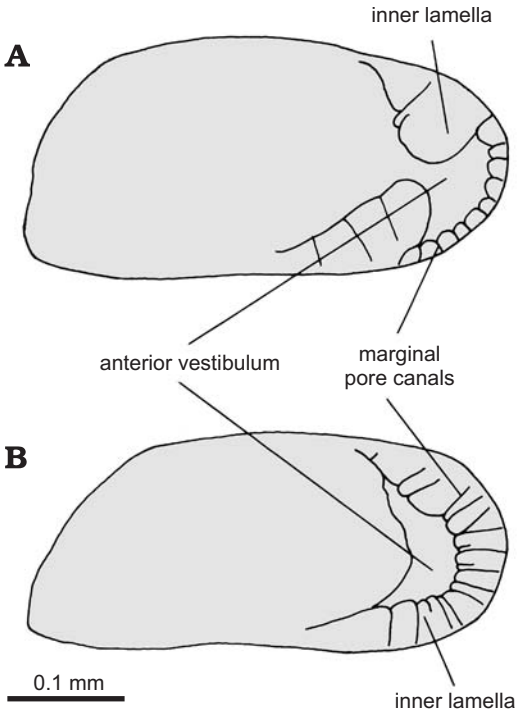

Fig. 4. Main morphological features of studied ostracods species. **A**. *Krithe iniqua* Abate, Barra, Aiello, and Bonaduce, 1993, right valve, transparence drawing from external view, sample 59, B.O.C. 2518, upper Pliocene, KI-29, sample 59. **B**. *Krithe compressa* (Seguenza, 1880), right valve, transparence drawing from external view, KC-29, sample 58, B.O.C. 2547, upper Pliocene.

the power law (1), the number C of pairs of points with distances smaller than R was plotted on a log-log scale as a function of R. The smallest distance has been chosen to be 1 μm, gradually increased by a factor of two. For all the available areal co-ordinates, the best fit of the least-squares regression line of log(C) on log(R), at confidence level higher than 99%, was obtained only within the scaling region of 4–2048 μm with a fractal dimension varying of 1.20–1.55. Half the lower limit value of the scaling region, equal to 2 μm, is related to the resolution of the vectorization process. The curvature of the log-log plot for R lower than 4 μm and for R greater than 2048 μm does not allow a direct interpretation of D. As R approaches the size of the investigated area there are fewer and fewer pairs of points with sufficient separation; for values of R greater than the size of the investigated area, no pairs are found and the number of pairs with distances less than R remains the same as R increases and D = 0 (due to the edge effect) (Fig. 5).

For geometric morphometrics analysis, we selected 12 landmarks (Fig. 6) on each drawing using Tps Dig 1.31 (Rohlf 2001a). Landmarks were chosen so as to capture overall valve shape and details of characters relevant to *Krithe* systematics (see Reyment 1993 for a similar procedure). Landmarked images were translated, rotated and scaled to the unit centroid size according to the generalized procrustes analysis (GPA). Relative warp (RW) scores of shape variables were then used to perform a relative warp analysis with Tps Relw 1.23 (Rohlf 2001b). MANOVA was applied to test for significant differences in shape data. RW scores were further analysed to investigate population-level differences as for one of the species under concern, *K. compressa*, we had three different samples under analysis. Sheffe multiple comparison tests were employed as for this analysis.

In addition to the methods presented above, we determined whether the samples belonged (statistically) to the same population, by comparing morphometric liner measurements (L, H, and D) by multivariate analysis of variance (MANOVA).

Finally, to test for potential differences in fractal measurements, a two-sample Kolmogorov-Smirnov (K-S) test was utilized. The K-S statistic is sensitive to any kind of difference in the distribution from which the two samples are drawn, thus we performed both K-S and Mann-Whitney tests. A five percent probability was considered as the level of rejection of the null hypothesis. All analyses were performed using the statistical package SPSS 13. We predicted that the variability of different samples of the same species would be smaller than that observed in samples of different species.

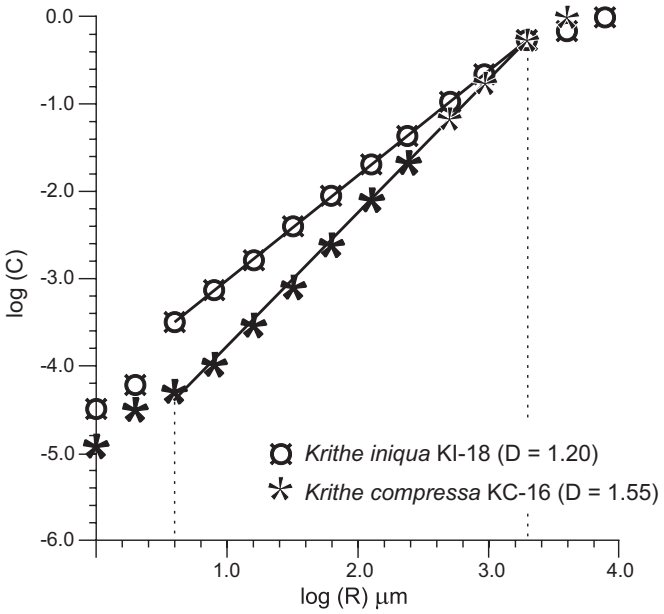

Fig. 5. The logarithm of number of pairs C of points with mutual distance smaller than R (μm), as a function of log(R). Vertical dashed lines are the limits inside which the linear slope of log(C) on log(R) provides the best fitting to the data.

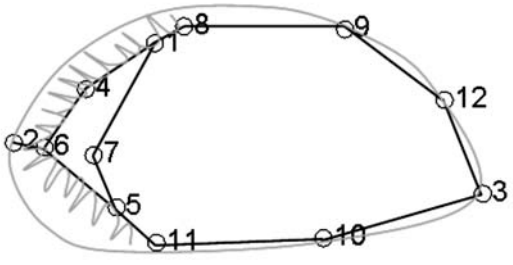

Fig. 6. Location of landmarks chose on *Krithe* valve for shape analysis.

Table 1. Fractal dimensions (D), length (L), and height (H) of the studied specimens of *Krithe iniqua* and *Krithe compressa*.

Krithe iniqua	D fractal	L	H
KI-01	1.30	0.557	0.253
KI-02	1.32	0.532	0.263
KI-03	1.34	0.552	0.248
KI-04	1.32	0.547	0.253
KI-05	1.31	0.542	0.258
KI-06	1.30	0.537	0.258
KI-07	1.34	0.527	0.243
KI-08	1.33	0.532	0.263
KI-09	1.30	0.542	0.273
KI-10	1.35	0.562	0.253
KI-11	1.32	0.537	0.243
KI-12	1.32	0.552	0.273
KI 13	1.34	0.562	0.253
KI-14	1.34	0.552	0.248
KI-15	1.31	0.552	0.273
KI-16	1.31	0.542	0.238
KI-17	1.31	0.537	0.263
KI-18	1.20	0.537	0.268
KI-19	1.31	0.552	0.243
KI-20	1.31	0.532	0.268
KI-21	1.31	0.537	0.248
KI-22	1.30	0.562	0.243
KI-23	1.32	0.522	0.268
KI-24	1.29	0.522	0.263
KI-25	1.30	0.527	0.263
KI-26	1.29	0.547	0.273
KI-27	1.28	0.537	0.268
KI-28	1.28	0.527	0.263
KI-29	1.31	0.547	0.268
n	29	29	29
min	1.2	0.522	0.238
max	1.35	0.562	0.273
average	1.31	0.54	0.26
standard deviation	0.0276	0.0118	0.0107

Krithe compressa	D fractal	L	H
KC-01	1.41	0.587	0.268
KC-02	1.39	0.577	0.273
KC-03	1.41	0.587	0.278
KC-04	1.37	0.567	0.263
KC-05	1.40	0.562	0.263
KC-06	1.41	0.557	0.263
KC-07	1.38	0.557	0.263
KC-08	1.33	0.567	0.268
KC-09	1.29	0.562	0.263
KC-10	1.37	0.557	0.263
KC-11	1.41	0.542	0.253
KC-12	1.42	0.557	0.263
KC-13	1.42	0.542	0.253
KC-14	1.38	0.547	0.285
KC-15	1.39	0.552	0.258
KC-16	1.55	0.572	0.268
KC-17	1.40	0.552	0.248
KC-18	1.40	0.557	0.268
KC-19	1.38	0.557	0.258
KC-20	1.36	0.547	0.253
KC-21	1.38	0.552	0.268
KC-22	1.40	0.562	0.263
KC-23	1.40	0.557	0.253
KC-24	1.40	0.552	0.258
KC-25	1.43	0.552	0.258
KC-26	1.40	0.522	0.248
KC-27	1.40	0.547	0.263
KC-28	1.40	0.532	0.253
KC-29	1.39	0.542	0.248
n	29	29	29
min	1.29	0.522	0.248
max	1.55	0.587	0.285
average	1.39	0.56	0.26
standard deviation	0.04067	0.0142	0.0088

Table 2. Two-sample Kolmogorov-Smirnov test and Mann-Whitney test statistic for pairwise comparisons of D fractal values of different samples of *Krithe compressa* and those of *Krithe iniqua*.

Comparisons	Kolmogorov-Smirnov test			Mann-Whitney test	
	samples	K-S	p	U	p
Krithe compressa sample 50 versus *K. compressa* sample 51	7, 11	0.564	0.908	38.0	0.964
Krithe compressa sample 50 versus *K. compressa* sample 58	7, 11	0.698	0.714	33.5	0.639
Krithe compressa sample 51 versus *K. compressa* sample 58	11, 11	0.853	0.461	59.5	0.946
Krithe iniqua versus *Krithe compressa* sample 50	29, 7	2.375	0.001	0.00	<0.001
Krithe iniqua versus *Krithe compressa* sample 51	29, 11	2.567	0.001	30.5	<0.001
Krithe iniqua versus *Krithe compressa* sample 58	29, 11	2.824	0.001	0.00	<0.001

Results and discussion

Results of the fractal analysis are summarized in Table 1. In order to evaluate morphological variations in *Krithe compressa* and *K. iniqua* we measured their lengths (L), heights (H) and fractal dimensions (D). We compared L and H of different samples of *K. compressa* (samples 50, 51, 58) between themselves and with *K. iniqua*. These comparisons indicate that when the four samples of the two species are considered, MANOVA shows highly significant differences (Wilk's

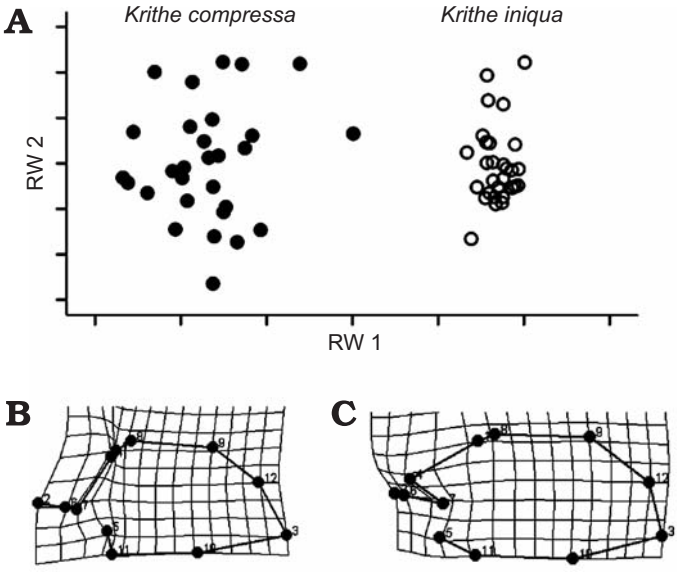

Fig. 7. RW1/RW2 plot showing the neat separation of *Krithe compressa* from *Krithe iniqua* specimens. Deformation grids along RW1 (set at values of –0.2 and 0.2) are reported. **A**. Plot of RW1 against RW2 scores. **B**, **C**. Shell deformation at extreme values along RW1.

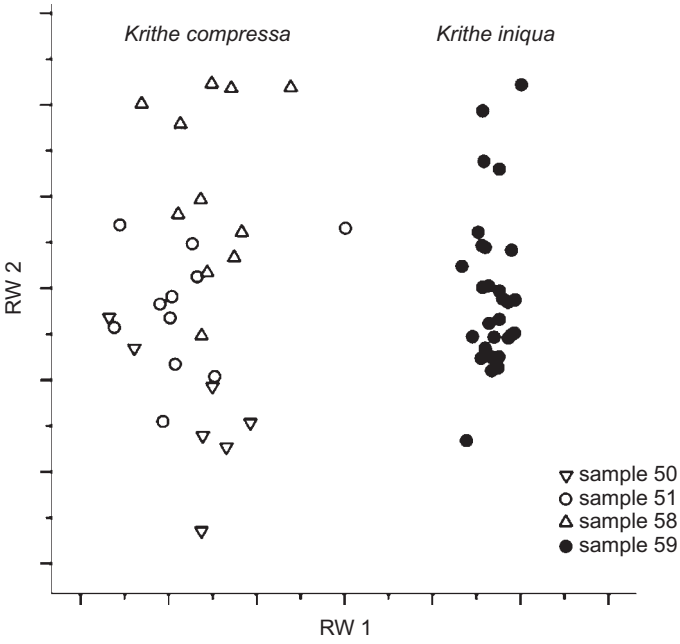

Fig. 8. This plot is the same as in Fig. 7, except for marks have been appended according to sample of provenance instead of species.

Table 3. Results of relative warp analysis.

RW	SV	%	Cum %
1	0.66305	78.95	78.95
2	0.16382	4.82	83.77
3	0.14757	3.91	87.68
4	0.13124	3.09	90.78
5	0.10675	2.05	92.82
6	0.09597	1.65	94.48

Lambda 0.249, F = 10.857, df = 9, P = 2.15×10^{-12}) among the samples. A test of between samples effects shows that only length and D are, however, significantly different among the four samples [L: F(3,54) = 8.558, p = 0.001; H: F(3,54) = 2.827, p = 0.068, NS; D: F(3,54) = 8.942, p <0.001]. Results of post-hoc pair-wise comparisons for L of different samples (and species) indicate that individuals of *K. compressa* in sample 58 are not distinguishable from those of *K. iniqua* and that individuals in sample 51 are not different from those of sample 58 of *K. compressa*.

On the other hand, fractal analysis of the two ostracod species shows values of D centered on 1.31±0.02 for *Krithe iniqua* and on 1.40±0.04 for *K. compressa* (Table 1). Also in this case we compared D values of *K. compressa* from different samples among themselves. No significant differences were found (Table 2). However, D values are significantly different when individuals of *K. iniqua* are compared with those of *K. compressa* (Table 2).

Geometric morphometrics indicates significant differences at the species level. Relative warp analysis indicates that clear morphological differences are present within species (Table 3, Fig. 7). Species are clearly separated along RW1, where the shape goes from the narrow (antero-posteriorly) vestibulum and highly slanted posterior margin of the valve typical of *K. compressa* to the mushroom-shaped vestibulum and less slanted posterior margin of *K. iniqua*. This finding agrees with traditional systematics in which this character is used for separating *K. compressa* and *K. iniqua*.

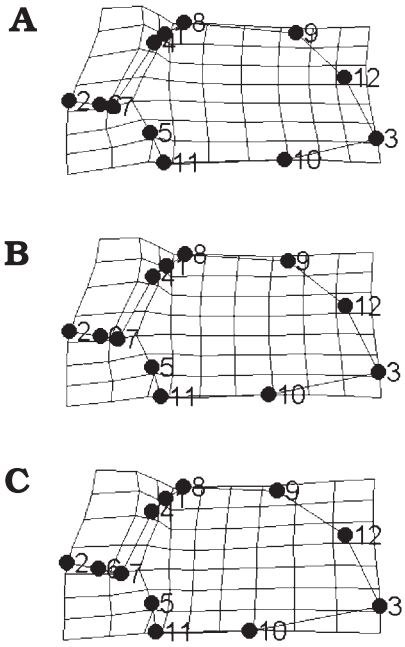

Fig. 9. Continuous shape variation in *Krithe compressa* valves drawn along RW 2. Deformation grids relate to specimen of the three different samples belonging to *Krithe compressa* from the highest (**A**) to the lowest (**C**) RW 2 scores (see Fig. 7). Deformation grid in B refers to undeformed shape. From the above, a valve from sample 58 (specimen KC 25), a specimen from sample 51 (KC 16), and a specimen from sample 50 (KC 1).

Table 4. Results of Scheffe multiple comparison test. Significant differences are marked with an asterisk.

Dependent variable	(I) sample	(J) sample	Mean difference (I–J)	Standard error	p	95% confidence interval	
						lower bound	upper bound
RW 1	50	51	0.0040	0.01021	0.985	–0.0255	0.0335
		58	–0.0113	0.01021	0.748	–0.0408	0.0182
		59	–0.1718*	0.00889	0.000	–0.1975	–0.1461
	51	50	–0.0040	0.01021	0.985	–0.0335	0.0255
		58	–0.0153	0.00901	0.418	–0.0413	0.0107
		59	–0.1758*	0.00748	0.000	–0.1974	–0.1542
	58	50	0.0113	0.01021	0.748	–0.0182	0.0408
		51	0.0153	0.00901	0.418	–0.0107	0.0413
		59	–0.1605*	0.00748	0.000	–0.1821	–0.1389
	59	50	0.1718*	0.00889	0.000	0.1461	0.1975
		51	0.1758*	0.00748	0.000	0.1542	0.1974
		58	0.1605*	0.00748	0.000	0.1389	0.1821
RW 2	50	51	–0.0229	0.00820	0.061	–0.0466	0.0007
		58	–0.0503*	0.00820	0.000	–0.0740	–0.0266
		59	–0.0264*	0.00715	0.006	–0.0470	–0.0058
	51	50	0.0229	0.00820	0.061	–0.0007	0.0466
		58	–0.0274*	0.00724	0.005	–0.0483	–0.0065
		59	–0.0035	0.00601	0.953	–0.0208	0.0139
	58	50	0.0503*	0.00820	0.000	0.0266	0.0740
		51	0.0274*	0.00724	0.005	0.0065	0.0483
		59	0.0239*	0.00601	0.003	0.0066	0.0412
	59	50	0.0264*	0.00715	0.006	0.0058	0.0470
		51	0.0035	0.00601	0.953	–0.0139	0.0208
		58	–0.0239*	0.00601	0.003	–0.0412	–0.0066

MANOVA indicates the differences to be statistically significant (Wilk's Lambda 0.18, df = 20, P = 1.63×10^{-026}). Sheffe multiple contrasts run on samples indicate differences to be significant at the species level on RW1 (Table 4). Interestingly, samples of *K. compressa* are statistically different along RW2 when contrasted with one another (Figs. 8, 9). Most variation along RW2 is dependent on vestibular area variability.

In summary: (1) The observed variability within populations, which is probably connected with environmental factors such as dissolved oxygen and food supply (Peypouquet 1975, 1977, 1979; Van Harten 1995, 1996; Corbari 2004), does not allow a distinction to be made between different taxa when simple measures such as L and H are considered as variability indicators; (2) Fractal analysis, however, is an important measure of individual variability and allows the distinction between different taxa since it is a representation of morphological complexity even when expressed in two-dimensions; (3) Geometric morphometrics performs as well as fractal geometry and allows some interplay with the traditional "naked-eye" approach.

Conclusion

The fractal dimension is an index that ranges continuously from zero (when all the data are distributed in a single point or in isolated points) through one (with all the data distributed along a line) up to two (when all the data are distributed homogeneously or randomly in a plane).

The two ostracod species analysed here can be distinguished from one another on the basis of qualitative characters even though they are similar in shell size (L and H). Fractal analysis provides a way to quantify these differences (Table 2). The reduction of the representation of the shape (from three to two dimensions, reduction of descriptive elements) does not limit the possibility of discriminating (morphologically) different taxa at the species level.

The two values, which are very different, suggest the possibility of an effective utilization of fractal geometry in the taxonomy of Ostracoda.

As illustrated in the present paper, a comparison between D values may be utilized to assess and quantify morphological differences between two species.

Similarly, geometric morphometrics works quite well in assessing within-species morphological differences. The analysis of *K. compressa* samples also allows the recognition of within-species differences.

Geometric morphometrics appears to be more powerful in detecting intraspecific shape differences. Conversely, fractal analysis seems most appropriate in cases of subtle difference between species belonging to the same genus (e.g., complexity of ornamentation). A potential caveat of fractal analysis is that very different structures can have very similar D values.

This supports the idea that fractal analysis is most appropriate in analyses of congeneric species. Special attention should be paid to homology. Geometric morphometrics operationally includes the use of both homologous (true landmarks) and operationally analogous (pseudolandmarks) shape indicators (i.a., Reyment 1993). Fractal analysis is free from the use of homologous structures. Although potentially misleading if comparing distantly-related organisms, this latter characteristic is welcome in cases of uncertain homology in closely-related species.

Our results encourage future developments and the integration of mathematically based approaches such as fractal geometry and geometric morphometrics to studies of taxa of higher hierarchical level.

Acknowledgement

We are grateful to Paul Taylor (Natural History Museum, London, UK) for linguistic adjustment. Gene Hunt (Department of Paleobiology, Smithsonian Institution, Washington, USA) gave us important advice that let us improve the manuscript. We are grateful to Mike Foote (Department of the Geophysical Sciences, University of Chicago, USA), Øyvind Hammer (Paleontological Museum, Oslo, Norway) for their helpful comments and precious advice. We are grateful to Loredana Pellecchia who helped us with the preparation of some figures.

References

Abate, S., Barra, D., Aiello, G., and Bonaduce, G. 1993. The genus *Krithe* Brady, Crosskey and Robertson, 1874 (Crustacea: Ostracoda) in the Pliocene–Early Pleistocene of the M. San Nicola Section (Gela, Sicily). *Bollettino della Società Paleontologica Italiana* 32: 349–366.

Adams, D.C., Rohlf, F.J., and Slice, D.E. 2004. Geometric morphometrics: ten years of progress following the "revolution". *Italian Journal of Zoology* 71: 5–16.

Aiello, G., Barra, D., and Bonaduce, G. 2000. Systematics and biostratigraphy of the Ostracoda of the Plio-Pleistocene Monte S. Nicola section (Gela, Sicily). *Bollettino della Società Paleontologica Italiana* 39: 83–112.

Ayress, M.A., Barrows, T., Passlow, V., and Whatley, R. 1999. Neogene to Recent species of *Krithe* (Crustacea: Ostracoda) from the Tasman Sea and off Southern Australia with description of five new species. *Records of the Australian Museum* 51: 1–22.

Bath, A. 1974. *Spectral Analysis in Geophysics*. 563 pp. Elsevier, Amsterdam.

Bold, W.A. van den 1946. *Contribution to the Study of Ostracoda with Special Reference to the Tertiary and Cretaceous Microfauna of the Caribbean Region*. 167 pp. Proefschrift Rijks Universiteit Utrecht, Amsterdam.

Bold, W.A. van den 1968. Ostracoda of the Yague Group (Neogene) of the Northern Dominican Republic. *Bulletins of American Paleontology* 54 (239): 1–106.

Bookstein, F.L. 1989. Principal warps: thin plate spline and the decomposition of deformations. *I.E.E.E. Transactions on Pattern Analysis and Machine Intelligence* 11: 567–585.

Bookstein, F.L. 1991. *Morphometric Tools for Landmark Data: Geometry and Biology*. 435 pp. Cambridge University Press, New York.

Boyajian, G. and Lutz, T. 1992. Evolution of biological complexity and its relation to taxonomic longevity in the Ammonoidea. *Geology* 20: 983–986

Brady, G.S., Crosskey, H.W., and Robertson, D. 1874. A monograph of the Post-Tertiary Entomostraca of Scotland including species from England and Ireland. *Annual Volumes (Monographs) of the Palaeontographical Society* 28: 1–232.

Bruner E. and Manzi, G. 2004. Variability in facial size and shape among North and East African human populations. *Italian Journal of Zoology* 71: 51–56.

Claridge, M.F., Dawah, H.A., and Wilson, M.R. 1997. Practical approaches to species concepts for living organisms *In*: M.F. Claridge, H.A. Dawah, and M.R. Wilson (eds.), *Species: the Units of Biodiversity*, 1–15. Chapman and Hall, London.

Coles, G.P., Whatley, R.W., and Moguilevsky, A. 1994. The ostracod genus *Krithe* from the Tertiary and Quaternary of the North Atlantic. *Paleontology* 37: 71–120.

Corbari, L. 2004. *Physiologie respiratoire, comportementale et morphofonctionnelle des ostracodes Podocopes et Myodocopes et d'un amphipode caprellidé profond. Stratégies adaptatives et implications évolutives*. 300 pp. M.Sc. thesis 2885, Université Bordeaux 1, Bordeaux.

Corbit, J.D. and Garbary, D.J. 1995. Fractal dimension as a quantitative measure of complexity in plant development. *Proceedings of the Royal Society of London B* 262: 1–6.

Cronquist, A. 1988. *The Evolution and Classification of Flowering Plants*. 555 pp. The New York Botanical Garden, New York.

Davenport, J., Pugh, P.J.A., and McKechnie, J. 1996. Mixed fractals and anisotropy in subantarctic marine macroalgae from South Georgia: implications for epifaunal biomass and abundance. *Marine Ecology Progress Series* 136: 245–255.

Dongsheng, L., Zhaobi, Z., and Binghong, W. 1994. Research into multifractal analysis of earthquake spatial distribution. *Tectonophysics* 233: 91–97.

Elewa, A. 2003. Morphometric studies on three ostracod species of the genus *Digmocythere* Mandelstam from the Middle Eocene of Egypt. *Palaeontologia Electronica* 6 (2): 1–11.

Elewa, A. 2004. *Morphometrics: Applications in Biology and Paleontology*. 263 pp. Springer Verlag, Heidelberg.

Grassberger, P. and Procaccia, I. 1983. Measuring the strangeness of strange attractors. *Physica D* 9: 189–208.

Ishizaki, K. 1966. Miocene and Pliocene ostracodes from the Sendai area, Japan. *Science Reports of the Tohoku University, series 2 (Geology)* 37: 131–163.

Kenkel, N.C. and Walker, D.J. 1996. Fractals in the biological sciences. *Coenoses* 11: 77–100.

Korvin, G., Boyd, D.M., and O'Dowd, R. 1990. Fractal characterization of the South Australian gravity station network. *Geophysical Journal International* 100: 535–539.

Luongo, G. and Mazzarella, A. 1997. On the clustering of seismicity in the Southern Tyrrhenian sea. *Annali di Geofisica* 40: 1–7.

Mandelbrot, B.B. 1983. *The Fractal Geometry of Nature*. 460 pp. Freeman, New York.

Mayden, R.L. 1997. A hierarchy of species concepts: the denouement in the saga of the species problem *In*: M.F. Claridge, H.A. Dawah, and M.R. Wilson (eds.), *Species: the Units of Biodiversity*, 381–424. Chapman and Hall, London.

Mayr, E. 1996. What is a species, and what is not? *Philosophy of Science* 63: 262–277.

Mazzarella, A. 1998. The time clustering of floodings in Venice and the Cantor dust method. *Theoretical and Applied Climatology* 59: 147–150.

McKenzie, K.G., Majoran, S., Emami, V., and Reyment, R.A. 1989. The *Krithe* problem—First test of Peypouquet's hypothesis, with a redescription of *Krithe praetexta praetexta* (Crustacea, Ostracoda). *Palaeogeography, Palaeoclimatology, Palaeoecology* 74: 343–354.

Nonnenmacher, T.F., Losa, G.A., and Weibel, E.R. 1994. *Fractals in Biology and Medicine*. 416 pp. Birkhauser, Boston.

Peypouquet, J.P. 1975. Les variations des caractères morphologiques internes chez les ostracodes des genres *Krithe* et *Parakrithe*: relation possible avec le teneur en O_2 dissous dans l'eau. *Bulletin de l'Institut de Géologie du Bassin Aquitaine* 17: 81–88.

Peypouquet, J.P. 1977. *Les ostracodes et la connaissance des paleomilieux profonds. Application au Cenozoïque de l'Atlantique nord-oriental*. 443 pp. Ph.D. thesis. Université de Bordeaux, Bordeaux.

Peypouquet, J.P. 1979. Ostracodes et paléoenvironnements. Méthodologie et application aux domaines profonds du Cénozoïque. *Bulletin du Bureau de Recherches Géologiques et Minieres* 4: 3–79.

Raia, P. 2004. Morphological correlates of tough food consumption in large land carnivores. *Italian Journal of Zoology* 71: 45–50.

Reyment, R.A. 1993. Ornamental and shape variation in *Hemicytherura fulva* McKenzie, Reyment and Reyment (Ostracoda, Eocene, Australia). *Revista Española de Paleontologia* 8: 125–131.

Reyment, R.A. 1995. On multivariate morphometrics applied to Ostracoda *In*: J. Ríha (ed.), *Ostracoda and Biostratigraphy*, 203–213. Balkema, Rotterdam.

Reyment, R.A. and Abe, K. 1995. Morphometrics of *Vargula hilgendorfii* (Müller). *Mitteilungen aus dem hamburgischen zoologischen Museum und Institut* 92: 325–336.

Rohlf, F.J. 2001a. *TpsDig: Thin Plate Spline Digitise. (Version 1.31)*. State University of New York, Stony Brook.

Rohlf, F.J. 2001b. *TpsRelw: Thin Plate Spline Relative Warp Analysis. (Version 1.22)*. State University of New York, Stony Brook.

Rohlf, F.J. and Slice, D. 1990. Extension of the procrustes method for the optimal superimposition of landmarks. *Systematic Zoology* 39: 40–59.

Seguenza, G. 1880. Le formazioni terziarie della provincia di Reggio (Calabria). *Atti della Reale Accademia dei Lincei, serie 3 (Memorie della classe di Scienze Fisiche, Matemetiche e Naturali)* 6: 3–446.

Stanley, H.E. 1992. Fractal landscapes in physics and biology. *Physica A* 186: 1–32.

Tatsumi, J., Yamauchi, A., and Kono, Y. 1989. Fractal analysis of plant root systems. *Annals of Botany* 64: 499–503.

Thompson, D'A.W. 1917. *On Growth and Form*. 793 pp. Cambridge University Press, Cambridge.

Van Harten, D. 1995. Differential food-detection: a speculative reinterpretation of vestibule variability in *Krithe* (Crustacea: Ostracoda) *In*: J. Ríha (ed.), *Ostracoda and Biostratigraphy*, 33–36. Balkema, Rotterdam.

Van Harten, D. 1996. The case against *Krithe* as a tool to estimate the depth and the oxygenation of ancient oceans *In*: A. Moguilewsky and R. Whatley (eds.), *Microfossils and Oceanic Environments*, 297–303. University of Wales, Aberystwyth.

Vlcek, J. and Cheung, E. 1986. Fractal analysis of leaf shapes. *Canadian Journal of Forest Research* 16: 124–127.

Whatley, R. and Zhao, Q. 1993. The *Krithe* problem: A case history of the distribution of *Krithe* and *Pararakrithe* (Crustacea, Ostracoda) in the South China Sea. *Palaeogeography, Palaeoclimatology, Palaeoecology* 103: 281–297.

Zhou, B. and Ikeya, N. 1992. Three species of *Krithe* (Crustacea : Ostracoda) from Suruga Bay, Central Japan. *Transactions and Proceedings of the Palaeontological Society of Japan, new series* 166: 1097–1115.